Electronic Supplementary Material (ESI) for Nanoscale Horizons.
This journal is © The Royal Society of Chemistry 2022

Supplemental Material to "Current Induced Hole Spin Polarization in Quantum Dot via Chiral Quasi Bound State"

The Supplementary Material includes the following topics:

S1. Hamiltonian and matrix elements

The Hamiltonian of the quantum dot (QD) with light holes side-coupled to the quantum wire with heavy holes can be written as follows [Eq. (1) in the main text]:

$$\mathcal{H} = E_0 \sum_{\pm} n_{\pm} + U n_+ n_- + \sum_{k,\pm} E_k n_{k,\pm} + \sum_{k,\pm} \left(V_{k,\pm} d_{\pm}^{\dagger} c_{k,\mp} + \text{H.c.} \right). \quad \text{(S1)}$$

We recall that $n_{\pm} = d_{\pm}^{\dagger} d_{\pm}$ are the occupancies of the light holes states in the QD having the spins $J_z = \pm 1/2$ with $d_{\pm}$ ($d_{\pm}^{\dagger}$) being the corresponding annihilation (creation) operators, E_0 is the energy of the light hole states in the QD which includes the interaction with the lower lying occupied heavy hole states in the QD, U is the Coulomb repulsion energy between the two light hole states, $n_{k,\pm} = c_{k,\pm}^{\dagger} c_{k,\pm}$ are the occupancies of the heavy hole states in the quantum wire with the wave vector k and spin $J_z = \pm 3/2$ with $c_{k,\pm}$ ($c_{k,\pm}^{\dagger}$) being the corresponding annihilation (creation) operators, and, finally, $V_{k,\pm}$ are the tunneling matrix elements.

The tunneling matrix elements $V_{k,\pm}$ can be calculated using the Luttinger Hamiltonian, which in the hole representation has the form [S1]:

$$\mathcal{H}_L = \begin{pmatrix} F & H & I & 0 \\ H^* & G & 0 & I \\ I^* & 0 & G & -H \\ 0 & I^* & -H^* & F \end{pmatrix}. \quad \text{(S2)}$$

It is written in the basis of the spin states $J_z = +3/2, +1/2, -1/2, -3/2$ and has the elements

$$\begin{aligned} F &= \frac{\hbar^2(\gamma_1 - 2\gamma_2)}{2m_0} k_z^2 + \frac{\hbar^2(\gamma_1 + \gamma_2)}{2m_0}(k_x^2 + k_y^2), \\ G &= \frac{\hbar^2(\gamma_1 + 2\gamma_2)}{2m_0} k_z^2 + \frac{\hbar^2(\gamma_1 - \gamma_2)}{2m_0}(k_x^2 + k_y^2), \\ H &= -\frac{\sqrt{3}\hbar^2 \gamma_2}{m_0} k_z (k_x - i k_y), \\ I &= -\frac{\sqrt{3}\hbar^2}{2m_0} \left[\gamma_2 (k_x^2 - k_y^2) - 2i\gamma_3 k_x k_y \right], \end{aligned} \quad \text{(S3)}$$

where m_0 is the free electron mass, $\gamma_{1,2,3}$ are the Luttinger parameters and $\boldsymbol{k}$ is the hole wave vector. We use the spherical approximation $\gamma_2 = \gamma_3$, so the Hamiltonian takes the form

$$\mathcal{H}_L = \frac{\hbar^2 k^2}{2m_0} \left(\gamma_1 + \frac{5}{2}\gamma_2 \right) - \frac{\hbar^2 \gamma_2}{m_0} (\boldsymbol{kJ})^2, \quad \text{(S4)}$$

where $\boldsymbol{J}$ is the hole spin. In this case the energy of the heavy hole states in the quantum wire reads

$$E_k = \frac{\hbar^2 k^2}{2m} \quad \text{(S5)}$$

with $m = m_0/(\gamma_1 + \gamma_2)$ being the heavy hole mass along the wire.

Let $\hat{\Psi}_{k,\pm} = \Psi_{k,\pm}\chi_{\pm 3/2}$ be the heavy hole wave function in the quantum wire with the wave vector k along the wire and the spin $J_z = \pm 3/2$ and $\hat{\Phi}_{\pm} = \Phi_{\pm}\chi_{\pm 1/2}$ be the light hole wave function in the QD with the spin $J_z = \pm 1/2$, respectively, where χ_{J_z} are the spinors. The tunneling matrix elements between them involve the change of the spin, which can not be provided by the external electrostatic potential. Instead, it is produced by the Luttinger Hamiltonian:

$$V_{k_\pm} = \left\langle \hat{\Phi}_{\pm} | \mathcal{H}_L | \hat{\Psi}_{k,\mp} \right\rangle. \quad \text{(S6)}$$

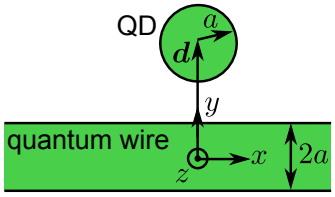

FIG. S1. Geometry of the system and the coordinate frame.

We assume that structure is symmetric in the (xy) plane containing the QD and the quantum wire, so the matrix elements between the states $\hat{\Phi}_\pm$ and $\hat{\Psi}_{k,\pm}$, respectively, being given by the H term in the Luttinger Hamiltonian, which is proportional to k_z, vanish. As a result, the coupling takes place between the states $\hat{\Phi}_\pm$ and $\hat{\Psi}_{k,\mp}$ only. It is produced by the matrix element I and involves the spin flip from $\mp 3/2$ to $\pm 1/2$, respectively.

To be specific, we consider the Gaussian wave functions [see Eqs. (3) in the main text]

$$\Phi_\pm = \varphi(z)\sqrt{\frac{2}{\pi}}\frac{1}{a}\exp\left(-\frac{x^2+(y-d)^2}{a^2}\right), \tag{S7a}$$

$$\Psi_{k,\pm} = -\psi(z)\sqrt{\frac{1}{aL}}\sqrt[4]{\frac{2}{\pi}}\exp\left(\mathrm{i}kx-\frac{y^2}{a^2}\right). \tag{S7b}$$

Here we use the coordinate frame with the origin at the center of the quantum wire cross section, we choose the x axis to be parallel to the quantum wire and the QD center to be located at the coordinates $(0,d,0)$, see Fig. S1. We assume the localization length a to be the same for the QD and the quantum wire, L is the normalization length, $\varphi(z)$ and $\psi(z)$ are the normalized wave functions along the growth axis z, and we assume the size quantization in this direction to be the strongest. The minus sign is introduced in Eq. (S7b) in order to get mostly positive tunneling matrix elements. We note that the matrix elements for the different localization lengths of the QD and the quantum wire can be also calculated analytically. However, we do not demonstrate it here since the corresponding expressions are cumbersome and all the physical effects do not change qualitatively.

For the wave functions (S7) the tunneling matrix elements read [Eq. (4) in the main text]

$$V_{k,\pm} = \frac{\sqrt{3}\sqrt[4]{2\pi}\gamma_2\hbar^2 V_z}{2m_0 a\sqrt{La}}\left[\left(\frac{d}{a}\pm ka\right)^2-1\right] \times\exp\left(-\frac{a^2k^2}{4}-\frac{d^2}{2a^2}\right), \tag{S8}$$

where $V_z = \langle\phi(z)|\psi(z)\rangle$. One can see, that the matrix elements are real. The matrix elements exponentially decay with the distance d between the QD and the quantum wire. Most importantly they are different for the given k, as illustrated in Fig. 2(a) in the main text. We note that the wave function (S7b) corresponds to the harmonic localization potential across the quantum wire along the y direction. In this case the energy of the state with the wave vector $k = 2/a$ coincides with the bottom of the second size quantized subband, so we will consider below the states in the range of $ka < 2$ only. In the same time, the ratio d/a can be arbitrary large in the model, but in fact it should not be too large in order to observe the effects of the hole tunneling between the QD and the quantum wire. We stress, that the tunneling matrix elements $V_{k,\pm}$ involve hole spin flips, but contain γ_2/γ_1 as a factor describing the spin-orbit interaction only. This ratio is not small, so the current induced spin polarization in this system is not parametrically suppressed.

For the given energy of the light hole states in the QD E_0 and the corresponding wave vector $k_0 = \sqrt{2mE_0}/\hbar$ the tunneling matrix elements are different $V_{k_0,+} \neq V_{k_0,-}$, which allows us to define chirality as follows [Eq. (5) in the main text] [S2–S4]:

$$\mathcal{C} = \frac{V_{k_0,+}^2 - V_{k_0,-}^2}{V_{k_0,+}^2 + V_{k_0,-}^2}. \tag{S9}$$

We note that due to the mirror and time reversal symmetries

$$V_{k,\pm} = V_{-k,\mp}, \tag{S10}$$

so the definition of the sign of $\mathcal{C}$ is arbitrary.

From Eq. (S8) we find the chirality

$$\mathcal{C} = \frac{4dk_0[(k_0a)^2+(d/a)^2-1]}{[(k_0a)^2-1]^2+6(dk_0)^2-2(d/a)^2+(d/a)^4}. \tag{S11}$$

One can see that it is an odd function of d and k_0 as shown in Fig. 2(b) in the main text. It vanishes at $d=0$ and $k=0$, as expected, and also at $(d/a)^2+(ka)^2=1$. These lines are white in Fig. 2(b) in the main text. But most importantly the chirality reaches ± 1 at [Eq. (6) in the main text]

$$k_0a = \pm d/a \pm 1, \tag{S12}$$

which is shown by yellow and light blue lines in Fig. 2(b) in the main text. Along these lines the current induced spin polarization can reach exactly 100%, as we demonstrate in the main text. We note that the corresponding energy E_0 can be found for any d, and we checked that this holds for a broad class of the wave functions apart from Eqs. (S7).

We note that the above expressions are based on the specific form of the wave functions, Eqs. (S7), which allows us to calculate the matrix elements (S8) analytically and simplifies all the calculations. The specific form of the matrix elements is not important and the large current induced hole spin polarization is possible for the other forms of the wavefunctions.

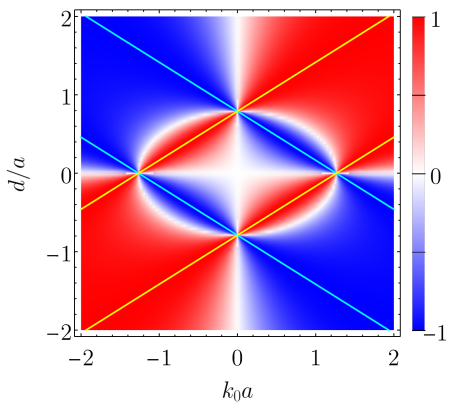

FIG. S2. Chirality $\mathcal{C}$ of the quasi bound state calculated after Eq. (S14) in the same axes and scale as in Fig. 2(b) in the main text.

To illustrate this, let us consider the wave function of the quantum dot with the localization length $a/2$:

$$\Phi_{\pm} \propto \exp\left(-\frac{x^2+(y-d)^2}{(a/2)^2}\right). \tag{S13}$$

In this case we obtain the chirality

$$\mathcal{C} = \frac{160dk_0[(5k_0a)^2+(8d/a)^2-40]}{[(5k_0a)^2-40]^2+6(40dk_0)^2-5(32d/a)^2+(8d/a)^4} \tag{S14}$$

instead of Eq. (S11). This expression is shown in Fig. S2, which is similar to Fig. 2(b) of the main text. One can see that the chirality is again of the order of unity almost in the whole range of the parameters, however the color map is squeezed.

The chirality in this case again reaches ±1 along the lines

$$5k_0a = \pm 8d/a \pm \sqrt{40}, \tag{S15}$$

which is an analog of Eq. (S12) in this case. These lines are shown in Fig. S2 as cyan and magenta lines. To understand the origin of the complete chirality let us consider the real matrix element $\left\langle \hat{\Phi}_{\pm}\middle|k_x+\mathrm{i}k_y\middle|\hat{\Psi}_{k,\mp}\right\rangle$. Here k_x can be replaced with k, so it is dominated by the k_x-related term in the limits $k\to\pm\infty$. However, in these two limits it has the opposite signs, so it unavoidably vanishes at some k. Similarly, the more complex matrix elements of $(k_x\pm\mathrm{i}k_y)^2$ in Eq. (S6) contain an interplay between k_x and $\mathrm{i}k_y$. Since the matrix element of $\mathrm{i}k_y$ is proportional to $1/a$ the signs of the total matrix elements $V_{k_0,\pm}$ change two times generally at k_0 of the order of $1/a$. Clearly, when one of the matrix elements vanishes the chirality, Eq. (S9), reaches its maximum ±1.

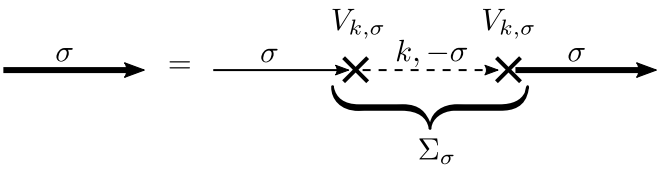

FIG. S3. Dyson equation and the self energy for the tunneling problem. Thick solid, thin solid and dashed lines correspond to $G_\sigma(\omega)$, $G_{0,\sigma}(\omega)$, and $G_{k,-\sigma}(\omega)$, respectively.

S2. General formalism for current induced spin polarization

Here we calculate the current induced spin polarization in the QD produced by the nonequilibrium distribution functions of the heavy holes in the quantum wire inherited from the attached leads. We assume that the occupancies of the states in the quantum wire are given by

$$\langle n_k\rangle = \theta(E_k)\left[\theta(E_F^L-E_k)\theta(k)+\theta(E_F^R-E_k)\theta(-k)\right], \tag{S16}$$

where E_F^L and E_F^R are the Fermi energies in the left and right leads, respectively, and $\theta(t)$ is the Heaviside step function. This distribution is relevant for the temperatures below the width of the quasi bound state.

At the first step, we neglect tunneling and use equations of motion to obtain the retarded Hubbard Green's function of the QD [S5, S6] [c.f. Eq. (7) in the main text]:

$$G^R_{0,\sigma}(\omega) = \frac{1-\langle n_{-\sigma}\rangle}{\omega-E_0+\mathrm{i}\delta} + \frac{\langle n_{-\sigma}\rangle}{\omega-E_0-U+\mathrm{i}\delta}, \tag{S17}$$

where we set $\hbar=1$ for brevity. We recall that it is defined as the Fourier transform of $-\mathrm{i}\left\langle\left\{d^\dagger_\sigma(0),d_\sigma(t)\right\}\right\rangle\theta(t)$. The average occupancies of the light hole spin states $\langle n_\sigma\rangle$ should be determined self consistently taking into account the tunneling processes.

Then we account for the tunneling as a perturbation while keeping the Fermi energies in the left and right leads, E_F^L and E_F^R, different. This can be done in the Keldysh formalism [S7–S9]. The self energy in this problem is trivial, see Fig. S3, it reads

$$\Sigma^R_\sigma(\omega) = \sum_k |V^2_{k,\sigma}| G^R_{k,-\sigma}(\omega), \tag{S18}$$

where

$$G^R_{k,\sigma}(\omega) = \frac{1}{\omega-E_k+\mathrm{i}\delta} \tag{S19}$$

is the retarded Green's function of heavy holes in the quantum wire. We note that the tunneling in Eq. (S1) flips the spin σ. From the Dyson equation, Fig. S3, we obtain

$$G^R_\sigma(\omega) = \frac{G^R_{0,\sigma}(\omega)}{1-G^R_{0,\sigma}(\omega)\Sigma^R_\sigma(\omega)}. \tag{S20}$$

We note that the retarded self energy $\Sigma^R_\sigma(\omega)$ in Eq. (S18) diverges at $\omega = -\mathrm{i}\delta$ and as a result one obtains a pole in $G^R_\sigma(\omega)$ at small negative real ω, which corresponds to the truly bound state. This state is generally present in the one dimensional problems with an impurity. We will assume that E_0 is large enough and will neglect the contribution of the true bound state to the current induced spin polarization. In this case, in the steady state the lesser Green's function defined as the Fourier transform of $\mathrm{i}\left\langle d^\dagger_\sigma d_\sigma(t)\right\rangle$ is given by

$$G^<_\sigma(\omega) = G^R_\sigma(\omega)\Sigma^<_\sigma(\omega)G^A_\sigma(\omega), \tag{S21}$$

where $G^A_\sigma(\omega) = [G^R_\sigma(\omega)]^*$ is the advanced Green's function and $\Sigma^<_\sigma(\omega)$ is the lesser self energy given by

$$\Sigma^<_\sigma(\omega) = \sum_k |V^2_{k,\sigma}| G^<_{k,-\sigma}(\omega), \tag{S22}$$

as follows from Fig. S3. The lesser Green's functions of the holes in the quantum wire are determined by the occupancies of the states:

$$G^<_{k,\sigma}(\omega) = 2\pi\mathrm{i}\,\langle n_k\rangle\,\delta(\omega - E_k), \tag{S23}$$

which are defined by the Fermi energies in the leads, see Eq. (S16). This gives the lesser self energy

$$\Sigma^<_\sigma(\omega) = 2\mathrm{i}\left[\Gamma_{L,\sigma}(\omega)n_L(\omega) + \Gamma_{R,\sigma}(\omega)n_R(\omega)\right], \tag{S24}$$

where

$$\Gamma_{L/R,\sigma}(\omega) = \pi\frac{D(\omega)}{4}V^2_{+k_\omega/-k_\omega,\sigma} \tag{S25}$$

are the tunneling rates with $D(\omega) = (L/\pi)\sqrt{2m/\omega}$ being the total density of states in the quantum wire including spin, $n_{L/R}(\omega) = \left\langle n_{+k_\omega/-k_\omega}\right\rangle$, and $k_\omega = \sqrt{2m\omega}$. We note that $\Gamma(\omega) = \Gamma_{L,\sigma}(\omega) + \Gamma_{R,\sigma}(\omega)$ determines the widths of the quasi bound states according to:

$$-\,\mathrm{Im}\left[\Sigma^R_\sigma(\omega)\right] = \Gamma(\omega), \tag{S26}$$

where we used Eq. (S18). It does not depend on spin, as follows from Eq. (S10). The tunneling rates $\Gamma_{L/R,\sigma}(\omega)$ can be also obtained from the Fermi golden rule.

Finally, the occupancies of the spin states in the QD $\langle n_\pm\rangle$ should be found self consistently as

$$\langle n_\sigma\rangle = -\mathrm{i}\int\limits_{-\infty}^{\infty} G^<_\sigma(\omega)\frac{\mathrm{d}\omega}{2\pi}, \tag{S27}$$

where the lesser Green's function is given by Eq. (S21) with the lesser self energy from Eq. (S24) and retarded and advanced Green's functions from Eq. (S20), which includes the same occupancies of the spin states through the Hubbard Green's function, Eq. (S17).

Ultimately, the spin polarization in the QD is given by

$$P = \frac{\langle n_+\rangle - \langle n_-\rangle}{\langle n_+\rangle + \langle n_-\rangle}. \tag{S28}$$

Below we consider the limits of zero and infinite Coulomb interaction and use the wide band approximation to obtain simplified expressions for the current induced spin polarization.

S3. Weak Coulomb interaction

Here for the purpose of illustration we consider the simple limit of $U = 0$, when the interaction between the holes in the QD can be neglected. In this limit the bare Green's function of the QD, Eq. (S17), reduces to

$$G^R_{0,\sigma}(\omega) = \frac{1}{\omega - E_0 + \mathrm{i}\delta}. \tag{S29}$$

Thus from Eq. (S20) we obtain

$$G^R_\sigma(\omega) = \frac{1}{\omega - \tilde{E}_0(\omega) + \mathrm{i}\Gamma(\omega)}, \tag{S30}$$

where

$$\tilde{E}_0(\omega) = E_0 + \mathrm{Re}\left[\Sigma^R_\sigma(\omega)\right] \tag{S31}$$

is the energy of the quasi bound state in the QD. Substituting it in Eq. (S21) and Eq. (S27) along with Eq. (S24) we obtain the occupancies of the spin states

$$\langle n_\pm\rangle = \int\limits_0^\infty \frac{2\Gamma(\omega)n_\pm(\omega)}{\left[\omega - \tilde{E}_0(\omega)\right]^2 + \Gamma^2(\omega)}\frac{\mathrm{d}\omega}{2\pi}, \tag{S32}$$

where

$$n_\pm(\omega) = \frac{\Gamma_{L,\pm}(\omega)n_L(\omega) + \Gamma_{R,\pm}(\omega)n_R(\omega)}{\Gamma(\omega)}. \tag{S33}$$

One can obtain the same result for the limit of negligible Coulomb interaction from the exact solution of a single particle problem. To explicitly demonstrate this, we consider the single particle eigenfunctions of the Hamiltonian (S1) with $U = 0$. They can be found following, for example, the original work of Fano [S10]. For the given energy $E > 0$ and spin σ of the light hole state, the two energy degenerate wave functions have the form

$$\Psi^\sigma_{1,2} = a_{1,2}\Phi_\sigma + \mathrm{v.p.}\int\limits_0^\infty \mathrm{d}E'\left[b^\sigma_{1,2}(E')\Psi_{k',-\sigma} + c^\sigma_{1,2}(E')\Psi_{-k',-\sigma}\right], \tag{S34}$$

where the coefficients are

$$a_1 = \frac{4\sin(\Delta)}{\pi D(E)Y_E}, \tag{S35a}$$

$$b_1^\sigma(E') = \frac{V_{k',\sigma}}{Y_E}\left[\frac{1}{\pi}\frac{\sin(\Delta)}{E-E'} - \cos(\Delta)\delta(E-E')\right], \tag{S35b}$$

$$c_1^\sigma(E') = \frac{V_{-k',\sigma}}{Y_E}\left[\frac{1}{\pi}\frac{\sin(\Delta)}{E-E'} - \cos(\Delta)\delta(E-E')\right], \tag{S35c}$$

$$a_2 = 0, \tag{S36a}$$

$$b_2^\sigma(E') = \frac{V_{-k',\sigma}}{Y_E}\delta(E-E'), \tag{S36b}$$

$$c_2^\sigma(E') = -\frac{V_{k',\sigma}}{Y_E}\delta(E-E') \tag{S36c}$$

with the following parameters: $\Delta = \arctan[\Gamma/(\tilde{E}_0 - E)]$, $Y_E = \sqrt{V_{k_E,\sigma}^2 + V_{-k_E,\sigma}^2}$ (it does not depend on σ) and $k' = \sqrt{2mE'}$.

We note that

$$\tilde{E}_0 = E_0 + \text{v.p.}\int_0^\infty \mathrm{d}E' \frac{D(E')Y_{E'}^2}{4(E-E')} \tag{S37}$$

and

$$\Gamma = \pi\frac{D(E)Y_E^2}{4} \tag{S38}$$

in agreement with Eq. (S18): $\Sigma_\sigma^R(E) = \tilde{E}_0 - E_0 - \mathrm{i}\Gamma$.

We also note that these eigenfunctions do not form a complete set, because any potential in one dimensional problem produces a bound state with a negative energy $E_b < 0$. The two Kramers degenerate truly localized states have the same form of Eq. (S34):

$$\Psi_0^\sigma = a_0^\sigma\Phi_\sigma + \text{v.p.}\int_0^\infty \mathrm{d}E' \left[b_0^\sigma(E')\Psi_{k',-\sigma} + c_0^\sigma(E')\Psi_{-k',-\sigma}\right]. \tag{S39}$$

Here the coefficients have the form

$$b_0^\sigma(E') = \frac{D(E')a_0V_{k'}^\sigma}{4(E_b-E')}, \qquad c_0^\sigma(E') = \frac{D(E')a_0V_{-k'}^\sigma}{4(E_b-E')}, \tag{S40}$$

and the coefficient a_0 should be determined from the normalization of these wave functions. The energy of these truly bound states can be found from the relation

$$E_b = E_0 + \int_0^\infty \frac{D(E')Y_{E'}^2}{4(E_b-E')}. \tag{S41}$$

One can see that the Green's function (S30) indeed has a pole at this energy. However, for $E_0 \gg \Gamma$ this state is almost delocalized, $a_0^\sigma \ll 1$, so the contribution of this state can be neglected.

For the simple Gaussian wave functions (S7) and matrix elements (S8) one can readily find the width of the quasi bound state

$$\Gamma = \frac{3\sqrt{\pi}\gamma_2^2\hbar^2mV_z^2}{2\sqrt{2}a^2m_0^2}\left[a^3k_E^3 + 2(3d^2/a^2-1)k_Ea + (d^2/a^2-1)^2/(k_Ea)\right]\exp\left(-k_E^2a^2/2 - d^2/a^2\right). \tag{S42}$$

For the energy renormalization we obtain

$$\tilde{E}_0 - E_0 = \frac{3\gamma_2^2\hbar^2mV_z^2}{2\sqrt{2}a^2m_0^2}\left\{2\left[(k_Ea)^3 + 2k_Ea(3d^2/a^2-1) + (d^2/a^2-1)^2/(k_Ea)\right]\mathcal{D}(k_Ea/\sqrt{2}) + \sqrt{2}\left[1 - 6(d/a)^2 - (k_Ea)^2\right]\right\}\exp\left(-d^2/a^2\right), \tag{S43}$$

where $\mathcal{D}(x) = e^{-x^2}\int_0^x \mathrm{e}^{y^2}\mathrm{d}y$ is the Dawson function. We remind that $k_E = \sqrt{2mE}/\hbar$ is used for brevity, and here we recovered the reduced Plank constant.

To describe the population of the QD spin states in the presence of the current, we consider the following linear combinations of the eigenfunctions at the given energy:

$$\Psi_L^\sigma = \frac{1}{Y_E}\left[V_{-k_E,\sigma}\Psi_2^\sigma - V_{k_E,\sigma}\mathrm{e}^{\mathrm{i}\Delta}\Psi_1^\sigma\right], \tag{S44a}$$

$$\Psi_R^\sigma = \frac{1}{Y_E}\left[V_{k_E,\sigma}\Psi_2^\sigma + V_{-k_E,\sigma}\mathrm{e}^{\mathrm{i}\Delta}\Psi_1^\sigma\right]. \tag{S44b}$$

These wave functions have the asymptotic behaviour $\Psi_{L/R}^\sigma \propto \exp(\pm\mathrm{i}k_Ex)$ for $x \to \pm\infty$, respectively. Thus they describe the heavy hole states propagating from the left and right leads, respectively.

The weight of the QD state in these functions is [S11]

$$|a_{L/R,\sigma}^2| = \frac{V_{\pm k_E,\sigma}^2}{(E-\tilde{E}_0)^2 + \Gamma^2}. \tag{S45}$$

For the given Fermi energies E_F^L and E_F^R in the leads (and low temperatures) the occupancies of the QD states can be found as

$$\langle n_\sigma\rangle = \int_0^{E_F^L}|a_{L,\sigma}^2|\frac{D(E)}{4}\mathrm{d}E + \int_0^{E_F^R}|a_{R,\sigma}^2|\frac{D(E)}{4}\mathrm{d}E, \tag{S46}$$

which coincides with Eq. (S32) obtained in the Keldysh formalism.

The tunneling matrix elements are exponentially suppressed by the fast decay of the hole wave functions away from the QD and the quantum wire. So typically the width of the resonance Γ is much smaller than its energy

E_0. The uncertainty of the wavevector k is of the order of

$$\frac{\Gamma m}{\hbar k_0} \sim \frac{1}{a}\frac{\Gamma}{\sqrt{\frac{\hbar^2}{ma^2}E_0}} \lesssim \frac{1}{a}\frac{\Gamma}{E_0}, \tag{S47}$$

which is much smaller than $1/a$. So one can use the wide band approximation and neglect the energy dependence of $D(E)$ and $V_{\pm k_E,\sigma}$ (this will be additionally illustrated in the next section). Then Eq. (S46) yields

$$\langle n_\pm\rangle = \frac{1}{2} + \frac{1\pm\mathcal{C}}{2\pi}\arctan\left(\frac{E_F^L-\tilde{E}_0}{\Gamma}\right) + \frac{1\mp\mathcal{C}}{2\pi}\arctan\left(\frac{E_F^R-\tilde{E}_0}{\Gamma}\right), \tag{S48}$$

where the chirality $\mathcal{C}$ is defined in Eq. (S9), while the quasi bound state energy $\tilde{E}_0$ and width Γ are assumed to be taken at the energy E_0.

One can see that the polarization is the largest in the limit of large bias $E_F^L - E_0, E_0 - E_F^R \gg \Gamma$. In this limit one has $\langle n_\pm\rangle = (1\pm\mathcal{C})/2$, which yields the polarization

$$P = \mathcal{C}. \tag{S49}$$

So the chirality directly defines the largest current induced spin polarization without interaction.

We note that the limit of the large bias can be also described using the phenomenological kinetic equations

$$\frac{\mathrm{d}n_\pm}{\mathrm{d}t} = 2\Gamma_{L,\pm} - 2\Gamma n_\pm, \tag{S50}$$

which describe the tunneling of the light holes to the QD with the rate $2\Gamma_{L,\pm}$ and out of the QD with the rate 2Γ. In the steady state one obtains once again $n_\pm = \Gamma_{L,\pm}/\Gamma = (1\pm\mathcal{C})/2$ and Eq. (S49) in agreement with the Keldysh formalism and exact Hamiltonian diagonalization.

S4. Strong Coulomb interaction

For small quantum dots it is relevant to consider the limit of strong Coulomb interaction, $U\to\infty$. In this limit one can neglect the second term in Eq. (S17) for the retarded bare Green's function $G^R_{0,\sigma}(\omega)$ [Eq. (7) in the main text]:

$$G^R_{0,\sigma}(\omega) = \frac{1-\langle n_{-\sigma}\rangle}{\omega - E_0 + \mathrm{i}\delta}. \tag{S51}$$

Similarly to the previous subsection we obtain the dressed retarded Green's function

$$G^R_{\sigma}(\omega) = \frac{1-\langle n_{-\sigma}\rangle}{\omega - E_{0,\sigma}(\omega) + \mathrm{i}\Gamma_\sigma(\omega)}, \tag{S52}$$

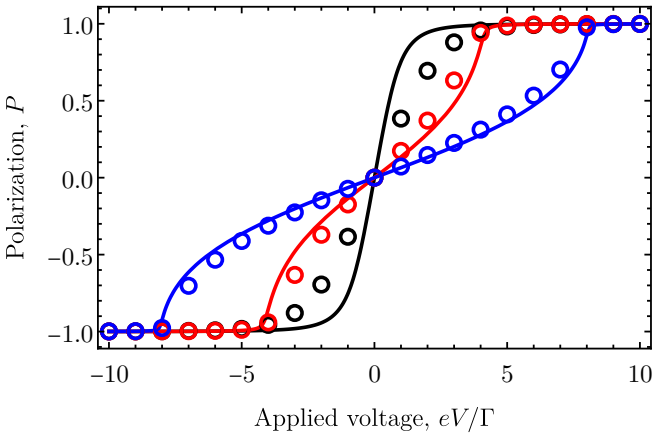

FIG. S4. Current induced spin polarization in the chiral bound state, $\mathcal{C}=1$, as a function of the applied bias, the same as in Fig. 3 in the main text. The black, red, and blue curves are calculated for $E_F - E_0 = 0$, 2Γ, and 4Γ, respectively, in the wide band approximation. The circles are calculated after Eq. (S27) without this approximation for $d/a = 3$, $k_0 a = 2$, $V_z = 1$, $\gamma_1 = 6.98$, and $\gamma_2 = 2.06$.

where $E_{0,\sigma}(\omega) = \langle n_{-\sigma}\rangle E_0 + (1-\langle n_{-\sigma}\rangle)\tilde{E}_0(\omega)$ and $\Gamma_\sigma(\omega) = (1-\langle n_{-\sigma}\rangle)\Gamma(\omega)$. Thus we obtain the suppressed amplitude of the Green's function, smaller renormalization of the energy of the quasi bound state, and its smaller width as compared with Eq. (S30).

Further, the occupancies of the QD spin states can be found from Eq. (S27) and (S21). In the wide band approximation in analogy with Eq. (S48) we obtain

$$\langle n_\sigma\rangle = (1-\langle n_{-\sigma}\rangle)\left[\frac{1}{2} + \frac{1+\sigma\mathcal{C}}{2\pi}\arctan\left(\frac{E_F^L-\tilde{E}_{0,\sigma}}{\Gamma_\sigma}\right) + \frac{1-\sigma\mathcal{C}}{2\pi}\arctan\left(\frac{E_F^R-\tilde{E}_{0,\sigma}}{\Gamma_\sigma}\right)\right]. \tag{S53}$$

This represents the set of two equations for $\langle n_\pm\rangle$, which should be solved self consistently.

The solution of these equations yield the current induced spin polarization according to Eq. (S28). The result of the calculation is shown in Fig. 3 in the main text. Note that these results are obtained in the wide band approximation, when the momentum dependence of the tunneling matrix elements is neglected. For comparison, we calculated the spin polarization also exactly after Eq. (S27) without the wide band approximation. The results are compared in Fig. S4. The main effect neglected in the wide band approximation is the renormalization of the quasi bound state energy from E_0 to $\tilde{E}_0$. This has a similar effect to the detuning of the Fermi energy E_F from the resonance energy E_0: It makes the saturation of the current induced spin polarization slower, but does not change the maximum value. Since the energy renormalization $\tilde{E}_0 - E_0$ is generally of the order of Γ, it has

almost no effect for $|E_F - E_0| \gg \Gamma$, as shown by the blue curve and blue circles in Fig. S4.

In the limit of large bias $E_F^L - E_0, E_0 - E_F^R \gg \Gamma$ one obtains

$$\langle n_\sigma \rangle = (1 - \langle n_{-\sigma} \rangle)(1 + \sigma \mathcal{C})/2, \tag{S54}$$

which yields [Eq. (12) in the main text]:

$$P_{\max} = \frac{2\mathcal{C}}{1 + \mathcal{C}^2}. \tag{S55}$$

Thus for the chiral quasi bound state, $\mathcal{C} = \pm 1$, in the presence of the interaction the current induced spin polarization reaches 100%.

This limit can be again described using the phenomenological kinetic equations

$$\frac{\mathrm{d}n_\sigma}{\mathrm{d}t} = 2\Gamma_{L,\sigma}(1 - n_{-\sigma}) - 2\Gamma n_\sigma, \tag{S56}$$

which is similar to Eq. (S50), but accounts for the Coulomb blockade effect. These equations lead to

$$n_\sigma = \frac{(1 \pm \mathcal{C})^2}{3 + \mathcal{C}^2}, \tag{S57}$$

which yields again Eq. (S55).

Generally, one can see that the Coulomb interaction increases the polarization degree. Qualitatively, this happens because the presence of a light hole with the given spin in the QD prevents tunneling of the hole with the opposite spin to the QD. As a result the spin polarization degree increases by a factor of $2/(1 + \mathcal{C}^2)$.

It follows from Eq. (S55) that it is enough to have quite a moderate chirality $|\mathcal{C}| > (10 - \sqrt{19})/9 \approx 0.63$ to obtain the spin polarization degree $P_{\max}$ larger then 90%. The corresponding region of the system parameters is shown in the inset in Fig. 4 in the main text.

To verify the applicability of our results to the non-Gaussian wave functions let us additionally consider

$$\Phi_\pm = \varphi(z)\sqrt{\frac{2}{\pi}\frac{1}{a}}\exp\left(-\frac{\sqrt{x^2 + (y-d)^2}}{a}\right), \tag{S58a}$$

$$\Psi_{k,\pm} = \psi(z)\sqrt{\frac{1}{aL}}\exp\left(\mathrm{i}kx - \frac{|y|}{a}\right). \tag{S58b}$$

These functions decay slower and seem to be more realistic than the Gaussian ones. However, the tunneling matrix elements for them can not be calculated analytically. Thus we performed the calculation of the current induced spin polarization completely numerically following the general expressions given above.

The maximum spin polarization $P_{\max}$ obtained in this way is shown in Fig. S5 as a function of the quasi bound state energy, $E_0/\mathcal{E}$, and distance between the quantum wire and the quantum dot, d/a. Quite surprisingly, the spin polarization turns out to be very large, much larger than for the Gaussian wave functions, c.f. the inset in Fig. 4 in the main text. We find that the maximum spin polarization is larger than 99.99% almost in the whole range of the system parameters under consideration. We additionally checked this surprising result by performing the same numerical calculations with the Gaussian wave functions (S7). The result was the same as in the inset Fig. 4 in the main text, which was calculated analytically. Thus the range of parameters suitable for the efficient current induced spin polarization is very broad independent of the specific form of the wave functions.

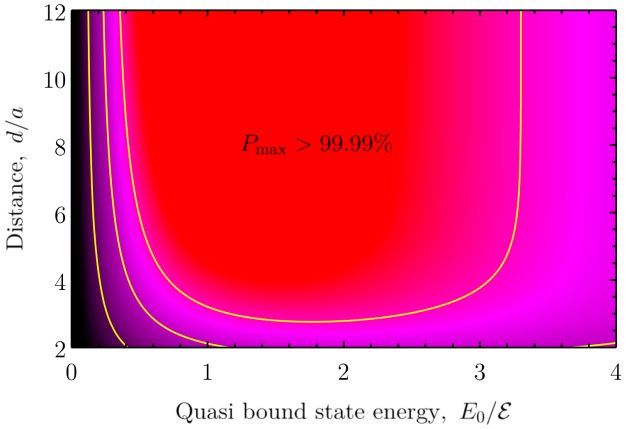

FIG. S5. Spin polarization in the limit of the large bias, $P_{\max}$, as a function of the quasi bound state energy E_0 and the distance between the QD and quantum wire. The yellow curves show the levels of $P_{\max} = 0.99$, 0.999 and 0.9999.

S5. Role of finite temperature

In all the above calculations the temperature T was set to zero, which is valid for $k_B T \ll \Gamma$, where k_B is the Boltzmann constant. In realistic systems, this can be a significant limitation for the application of our theory, so in this section we study the effect of the finite temperature.

This can be easily done in the framework of the Keldysh diagram technique: It is enough to modify only the occupancies of the states in the leads as follows:

$$\langle n_k \rangle = \theta(E_k)\left\{\frac{\theta(k)}{1 + \exp\left[(E_k - E_F^L)/(k_B T)\right]} + \frac{\theta(-k)}{1 + \exp\left[(E_k - E_F^R)/(k_B T)\right]}\right. \tag{S59}$$

In the limit of $T \to 0$ this expressions tends to Eq. (S16), which was used previously. Then the whole formalism of Sec. S2 remains the same.

In particular, in the limit of the strong Coulomb inter-

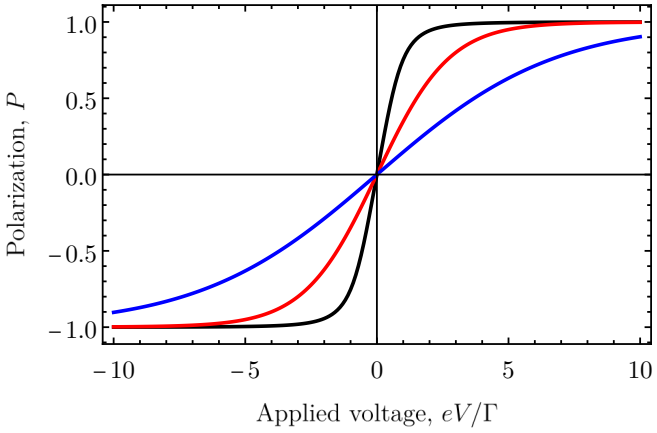

FIG. S6. Current induced spin polarization in the chiral bound state, $\mathcal{C} = 1$, as a function of the applied bias for the Fermi energy $E_F - E_0$ and different temperatures: $T = 0$ (black curve), Γ/k_B (red curve), and $3\Gamma/k_B$ (blue curve). The black curve coincides the black curve in Fig. 3 in the main text.

action, $U \to \infty$ we obtain instead of Eq. (S53)

$$\langle n_\sigma \rangle = \frac{1 - \langle n_{-\sigma} \rangle}{2\pi} \int\limits_{-\infty}^{\infty} \left\{ \frac{1 + \sigma\mathcal{C}}{1 + \exp\left[(E - E_F^L)/(k_B T)\right]} + \frac{1 - \sigma\mathcal{C}}{1 + \exp\left[(E - E_F^R)/(k_B T)\right]} \right\} \frac{\Gamma_\sigma}{(E - E_0)^2 + \Gamma_\sigma^2} \mathrm{d}E, \tag{S60}$$

where the quasi bound state energy renormalization is neglected.

The current induced spin polarization calculated from the solution of these two equations is shown in Fig. S6 for the completely chiral bound state, $\mathcal{C} = 1$, for the different temperatures. One can see that the temperature makes the polarization saturation smoother, but does not change its maximum value. Generally, the maximum spin polarization (S55) is reached when $eV \gg \Gamma$, $|E_F - E_0|$, and $k_B T$. In this limit, the quasi bound state coupling to the leads is determined by the chirality only. Thus the large current induced spin polarization is possible also for the finite temperature even when the thermal energy exceeds the width of the quasi bound state.

* Electronic address: smirnov@mail.ioffe.ru

[S1] E. L. Ivchenko, *Optical spectroscopy of semiconductor nanostructures* (Alpha Science, Harrow UK, 2005).

[S2] P. Lodahl, S. Mahmoodian, S. Stobbe, A. Rauschenbeutel, P. Schneeweiss, J. Volz, H. Pichler, and P. Zoller, Chiral quantum optics, Nature **541**, 473 (2017).

[S3] F. Spitzer, A. N. Poddubny, I. A. Akimov, V. F. Sapega, L. Klompmaker, L. E. Kreilkamp, L. V. Litvin, R. Jede, G. Karczewski, M. Wiater, T. Wojtowicz, D. R. Yakovlev, and M. Bayer, Routing the emission of a near-surface light source by a magnetic field, Nat. Phys. **14**, 1043 (2018).

[S4] A. Overvig, N. Yu, and A. Alù, Chiral Quasi-Bound States in the Continuum, Phys. Rev. Lett. **126**, 073001 (2021).

[S5] J. Hubbard and B. H. Flowers, Electron correlations in narrow energy bands, J. Proc. Roy. Soc. A **276**, 238 (1963).

[S6] H. Haug and A.-P. Jauho, *Quantum kinetics in transport and optics of semiconductors*, Vol. 2 (Springer, 2008).

[S7] J. Rammer and H. Smith, Quantum field-theoretical methods in transport theory of metals, Rev. Mod. Phys. **58**, 323 (1986).

[S8] G. Stefanucci and R. van Leeuwen, *Nonequilibrium Many-Body Theory of Quantum Systems: A Modern Introduction* (Cambridge University Press, 2013).

[S9] P. I. Arseev, On the nonequilibrium diagram technique: derivation, some features, and applications, Phys. Usp. **58**, 1159 (2015).

[S10] U. Fano, Effects of Configuration Interaction on Intensities and Phase Shifts, Phys. Rev. **124**, 1866 (1961).

[S11] P. W. Anderson, Localized Magnetic States in Metals, Phys. Rev. **124**, 41 (1961).